Diode-array detection in capillary electrophoresis using Agilent Extended Light Path capillaries

Technical Note

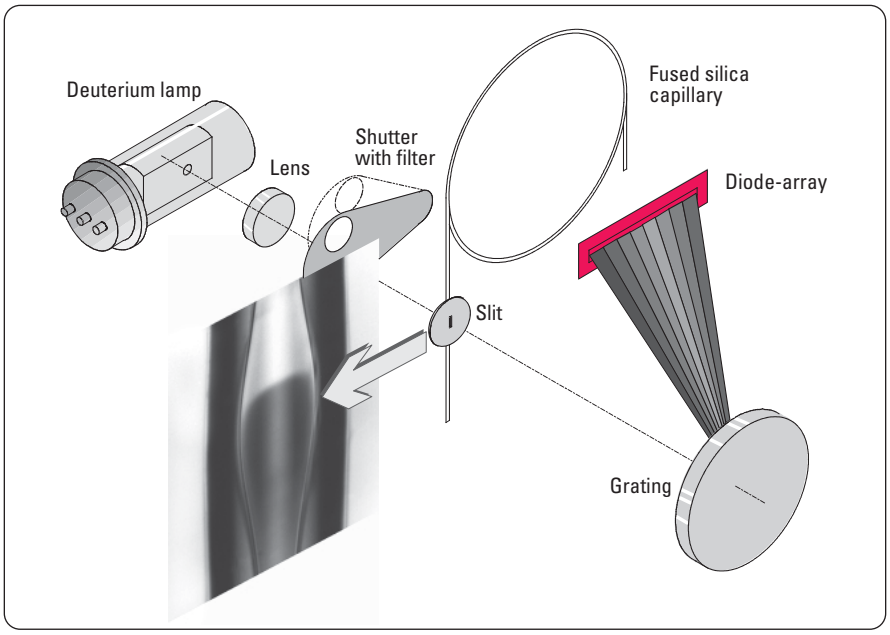

Overview

Detection in CE presents a number of challenges. These primarily result from the short optical pathlength of the narrow internal diameter capillaries employed, which typically range from 25 to 75 µm. Further, the oncapillary nature of the detection system makes it imperative to employ a detector specifically designed for use in CE and not simply a modified HPLC detector, to obtain high sensitivity and a large linear dynamic range.

Agilent Technologies

Introduction

The trend towards narrower diameter capillaries makes detection in CE more complex. Decreasing the internal diameter greatly reduces Joule heating and allows the application of high electric fields and the use of highly conductive buffers. This approach is fundamentally superior because it relies on minimization of heat generation rather than removal of heat after the fact. Capillaries down to 25-µm id offer these benefits but often demonstrate poor sensitivity.

Increasing the optical pathlength by simply using larger internal diameter capillaries, however, is not desirable due to the increased current and associated heating. Since current generation is proportional to the square of the inner diameter, increasing the internal diameter by a factor of three, for example, will raise current and heat nine times. Special capillary designs, such as Agilent Extended Light Path capillaries provide a unique solution to this problem.

Theory

On-capillary detection often uses designs such as that shown in figure 1, where a small portion of the capillary is illuminated with light from a UV light source and an optical aperture or slit behind the capillary is used to prevent stray light from reaching the detector.

The volume of the detection region is described by the three perpendicular axes of the capillary. (R) denotes the axial dimension of the slit and is also referred to as the height of the slit. It primarily affects electrophoretic resolution and light throughput. (O) is the radial dimension defined by the width of the slit. It determines the optical resolution of the system, governs the light throughput, and limits stray light. Lastly, (P), which is perpendicular to both (R) and (O), defines the optical pathlength of the detector region and thus the concentration response.

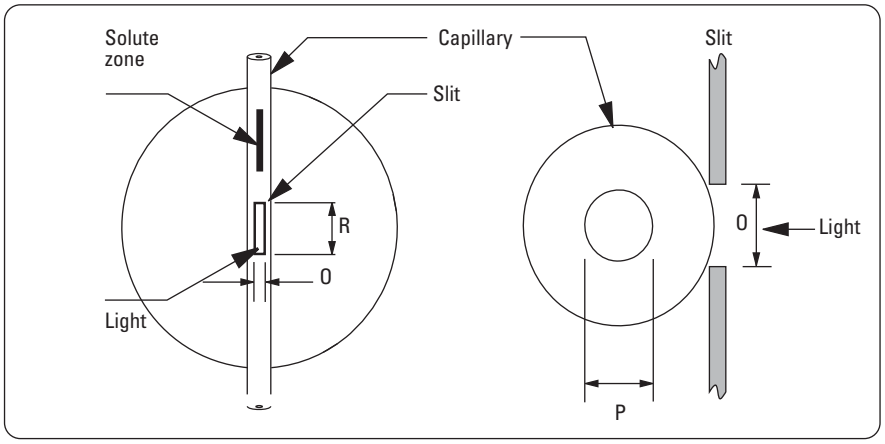

Figure 1
Positioning of the optical slit relative to the capillary.
R = slit height (along separation axis), O = slit width (perpendicular to R), P = pathlength.

The detection signal is primarily dependent on the pathlength. It is, however, also affected by the dimensions of the slit in the (O) dimension. Illuminating the whole cross section of the capillary by opening the slit in this dimension will actually decrease signal height. This is due to the circular geometry of the capillary which results in optical path lengths shorter than the internal diameter at the center. The effective pathlength for a circular cross section is actually 78.5 % (= 100 p/4) of the actual diameter. Using slit widths larger than the capillary internal diameter (O dimension) reduces the signalto- noise ratio, increases stray light and decreases linearity.[1] For this reason, it is imperative to match the optical slit with the inner diameter of the capillary. This is accomplished in the Agilent CE system by use of capillary interfaces which both align the capillary detection window and contain different slits for a variety of internal diameters. Sensitivity can also be improved by reducing baseline noise. Noise can be reduced by increasing the magnitude of light reaching the detector. The reduction is inversely proportional to the square root of the light intensity. This can be accomplished by using highintensity lamps and by maximizing the illuminated volume of the detection region. Increasing the slit width (O dimension) beyond the capillary internal diameters can be counterproductive because, as mentioned above, the signal will also decrease. The dimension of the optical slit is also constrained in the R dimension by the need to preserve the electrophoretic resolution of the narrow, closely spaced peaks often achieved in CE.

Agilent Extended Light

Path capillary ("bubble cell") A unique solution to improve detection in CE is the Agilent Extended Light Path capillary, shown in the photograph in figure 2. The inner diameter of this capillary is typically expanded three- to five-fold at the point of detection. The expanded section is often referred to as a "bubble cell". Due to electrophoretic phenomena, the increase in sensitivity is proportional to the increase in inner diameter. Importantly, there is no mixing or band broadening and virtually no loss of resolution. Additional advantages include improved detector linearity and, in some cases, decreased baseline noise.

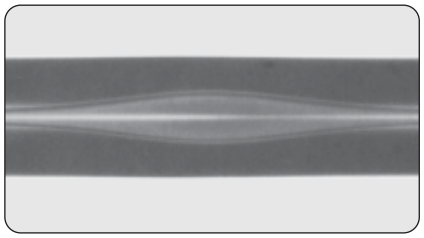

Figure 2
Photograph of 25-µm id capillary with 125 µm bubble cell.

While the bubble cell has a volume considerably larger than would be found in the same section of a standard capillary, resolution remains virtually unaffected due to reversible band compression in the axial direction (R dimension) resulting from the temporary decrease in electric field strength inside the bubble cell. The band compression is proportional to the square of the diameter at any given section of the bubble cell, leading to peaks that are compressed by a factor of nine to 25 for typical bubble cell dimensions of three to five times the capillary internal diameter.

Together with the axial compression (in the R dimension) in the bubble cell, the zone expands radially (in the O and P dimensions) to fill the increased area. The magnitude of this expansion is equivalent to the compression.The overall process, in a bubble cell with a threefold enlarged diameter, forms a zone that is three times longer in the P dimension, nine times narrower in the R dimension, and the same concentration as prior to entering the bubble region. By a similar process, the zone returns to its original state after it exits the bubble cell. Importantly, no turbulent flow, laminar flow, or other zonebroadening mechanism occurs in the bubble region. This is primarily due to the electroosmotic nature of the bulk flow of solution which is generated at the walls. In contrast, externally generated flow, for instance from an HPLC pump, will cause laminar flow and zone distortion.

Additionally, there are no adverse effects from Joule heating within the bubble cell because both the electric field and quantity of heat generated are proportionally lower in the region of the bubble.
A potential source of resolution loss comes not from zone broadening but from zone compression. This phenomenon is dependent only on the geometry of the optical slits used to define the detection "cell" dimensions.

Figure 3a, shows two snapshots of a straight capillary with a pair of closely eluting peaks traversing the detection cell. The first peak passes through the cell at time t_1, which is defined by the capillary diameter and the slit dimensions. As can be seen, the peak volume is larger than the cell volume. This allows for adequate resolution between this peak and the next peak, shown to be entering the cell at t2 just after the first peak has migrated completely out of the cell.

In figure 3b, the same two peaks are shown traversing a bubble cell with a threefold increase in diameter. The compression is quite apparent, as is the fact that the cell volume, defined by the same slit as used in the standard capillary, is now larger than the peak volume. Consequently, the second peak has already entered the detection area at t_2 while the first peak is still resident, leading to loss of resolution.

If the slit dimensions are adjusted to shorten the length of the detection region in the R dimension, as demonstrated in figure 3c, resolution equivalent to that of the straight cell is restored.

Resolution with the bubble cell capillary is identical to that of the standard capillary when the slit dimension in the R direction is reduced appropriately. In order to maintain optimal light throughput, however, the slit lengths employed are slightly larger than calculated from the theoretical compression of the solute zone. Slight loss of resolution (typically less than 5 %), when observed, can be attributed to this.

In practice, resolution is often unaffected because the zone broadening resulting from other factors often exceeds that caused by the dimensions of the bubble cell and the slit. The actual slit dimensions used are given in table I.

The maximum bubble factor that can be used in a capillary is primarily limited by the zone compression. Larger bubble cells require increasingly narrower slits (R dimension) to maintain resolution. For example, a 10 times

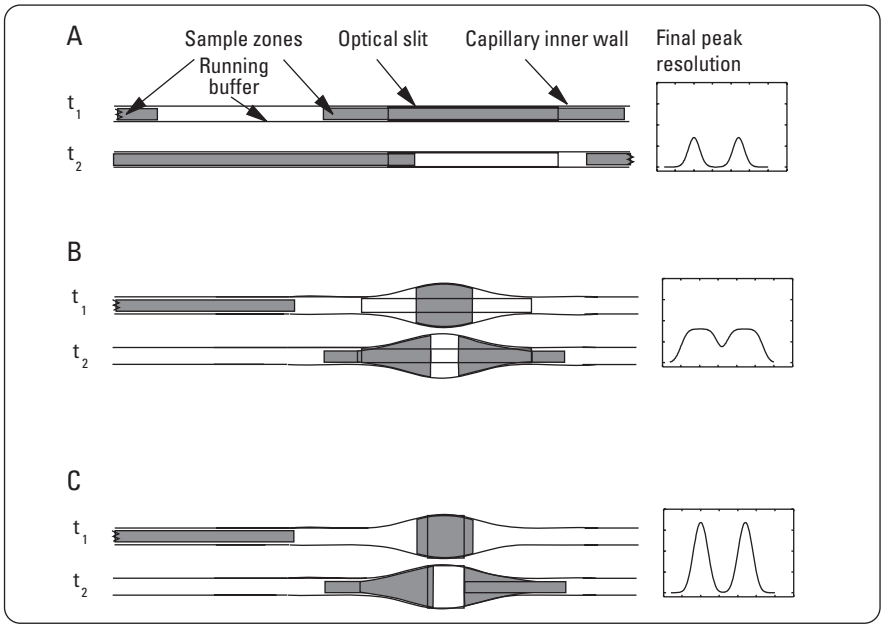

Figure 3
Band compression in the bubble cell and optimization of slit dimensions to maintain electrophoretic resolution.
A) standard capillary with standard slit dimensions
B) bubble cell capillary with standard slit dimensions
C) bubble cell capillary with bubble cell slit dimensions.

bubble factor in a 50-µm id capillary would require an optical slit of approximately 6.2 µm (= 620 µm/10^2) to maintain resolution relative to a standard capillary in an Agilent CE system. The minimal light throughput and high baseline noise associated with this configuration would negate the gain in signal from the increased optical pathlength. For this reason, the practical upper limit to the bubble factor is about five to six relative to the capillary inner diameter. Another advantage of the bubble cell is that it is essentially independent of the overall capillary internal diameter. This allows the use of narrow capillaries, (25-µm or less) with no detrimental effects to detection. In contrast, special capillary designs such as the "Z-cell" are limited to internal diameters of 75-µm or larger due to difficulties with light throughput. The "square" bubble cell slit offers an additional advantage over the standard "rectangular" slit. Because actual light intensities across the slit are not distributed uniformly but follow a Gaussian distribution, slits with a square cross section have better light throughput than rectangular slits of equivalent area.

Experimental

Capillary electrophoresis

Capillary electrophoresis experiments were performed on an Agilent CE system with built-in diode-array detector and Agilent ChemStation. Fused silica capillaries of 25-µm, 50-µm, and 75-µm inner diameter (id) and an outer diameter of 375 µm were used. The Agilent Extended Light Path capillaries had dimensions of 25-µm id with a bubble cell internal diameter of 125 µm, 50-µm id with a bubble cell diameter of 150 µm, and 75-µm id with a bubble cell diameter of 225 µm. Alignment interfaces containing optical slits matched to each capillary internal diameter were used. All interfaces and capillaries were supplied by Agilent Technologies. The term "bubble factor" or "BF" is used to describe the increase in capillary diameter relative to the standard capillary. A capillary with the diameter increased three times at the point of detection is denoted as BF 3. For example, the inner diameter of a 50-µm capillary with a three-fold expanded detection region is denoted 50-µm BF 3.

Inner diameter	Optical slit dimensions (R x O)* (slit incorporated into optical interface)
25 µm BF 5	80 x 120 µm
50 µm	620 x 40 µm
50 µm BF 3	145 x 145 µm
75 µm	620 x 55 µm
75 µm BF 3	150 x 200 µm

*R = height, along separation axis, O = width, orthogonal to R axis (figure 1), BF = bubble factor

Table I
Capillary internal diameter and slit dimensions for the Agilent CE system.

Chemicals and reagents

Reagents were of the highest grade possible and were purchased from Sigma Chemical Company (St Louis, MO, USA). All buffer solutions were filtered through a 0.2-µm membrane filter prior to use. HPLC grade solvents were obtained from Fisher Scientific (Springfield, NJ, USA). Detailed experimental conditions are included in the figure captions.

Results and discussion

Use of the bubble cell capillaries in a variety of applications and a comparison with the performance of standard capillaries is presented in this section. Data is shown to illustrate the effect of the bubble cell on sensitivity, resolution, efficiency, and linear dynamic range, as well as giving representative detection limits of the diodearray detector.

50- and 75-µm id bubble cell capillaries

A capillary zone electrophoresis separation of four neuropeptides is shown in figure 4. Using a buffer consisting of 30 mM boratephosphate, pH 8, the peptides were baseline resolved in about 5 minutes in a standard 50-µm id capillary (figure 4a). A reasonable signal-to-noise ratio was obtained for these compounds which were at a concentration of 10^{-5} M using a detection wavelength of 200 nm. The same separation was then performed using a bubble cell capillary of dimensions 50-µm BF 3 (figure 4b). Note that the

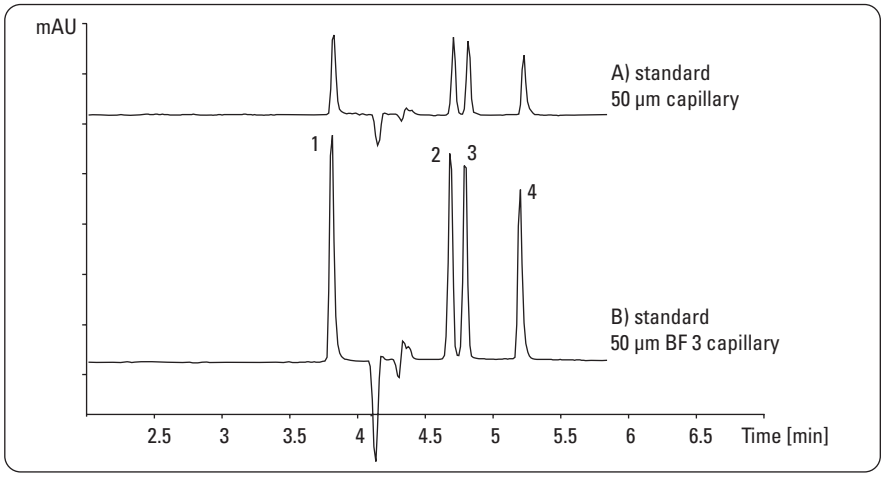

Figure 4
Peptide analysis using 50-µm id capillaries.

Chromatographic conditions

Samples:	1=neurotensin, 2=angiotensin II, 3=angiotensin I. 4=[leu]enkephanlin 10^{-5} M each
Buffer:	89 mM TRIS, 89 mM borate, pH 8.2
Capillary:	id=50 µm and 50 µm BF 3 (150 µm pathlength) l=56 cm; L=64.5 cm
Injection:	200 mbar x s
E:	370 V/cm
Temperature:	25 °C
Detection wavelength/bandwidth: 200/16 nm	

signal improved nearly three times, in proportion to the increase in inner diameter. Importantly, the resolution of angiotensin I and angiotensin II (peaks 2 and 3), which were just baseline resolved in the standard capillary, remained essentially unchanged with the bubble cell. Next protein digests were used to examine the characteristics of the bubble cell. Peptide mapping often presents a difficult separation due to the large number of peptides derived from the digestion of a protein.

An example of peptide mapping is shown in figure 5. Here, 0.5 mg/mL of carbonic anhydrase was digested with trypsin and analyzed using both standard 50-µm and 50-µm BF 3 capillaries. The peak patterns are nearly identical with both capillaries. The slight degradation in resolution in some regions of the electropherogram and improvement in other areas suggest that some of these inconsistencies may be attributed to the different capillary batches that were used for two capillaries and the run-to-run variations in the pattern, as well as to the possible influence of the bubble cell. Nonetheless, the 300 % gain in signal often outweighed the slight loss of resolution.

The bubble cell was then used to improve sensitivity for the analysis of organic acids using indirect UV detection. With this technique, non- or minimally-absorbing solutes are detected indirectly by displacement of the highly absorbing background electrolyte ion. The electropherograms of organic acids in diluted beer samples are shown in figure 6. For these analyses, phthalate was used as the indirect detection buffer because it strongly absorbed at 210 nm. In addition, the mobility of phthalate matches the mobility of many organic acids and yields good peak shapes. While indirect detection results in "negative" peaks, switching the signal and reference wavelengths of the diode-array detector inverts the peaks to the normal "positive" direction. The electropherograms show that the bubble cell,

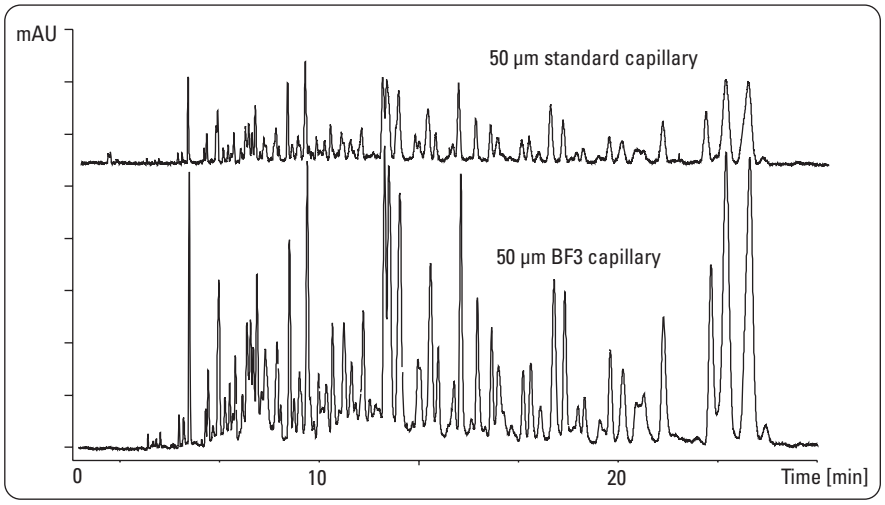

Figure 5
Comparison of standard and bubble cell capillaries in peptide mapping.

Chromatographic conditions

Sample:	0.5 mg/mL tryptic digest of carbonic anhydrase
Buffer:	20 mM phosphate, pH 3.0
Capillary:	id=50 µm BF 3 (150 µm pathlength); l=56 cm; L=64.5 cm
Injection:	50 mbar x s
E:	370 V/cm
Temperature:	25 °C

Detection wavelength/bandwidth: 200/16 nm

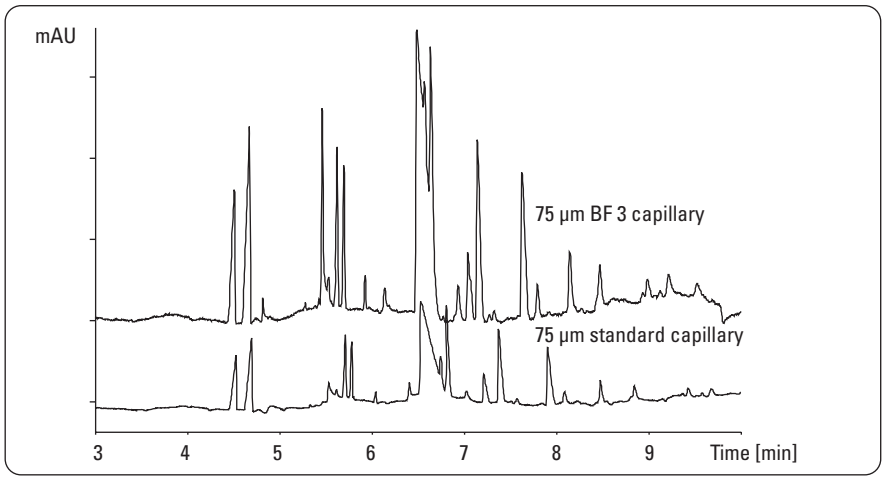

Figure 6
Standard and bubble cell capillaries for indirect detection of organic acids in beer. (Variations in migration times again result from differences in both capillary conditioning and capillary batches.)

Chromatographic conditions

Sample:	1:10 dilution of Hoepfner Pilsner (Germany)
Buffer:	5 mM phthalate, 0.25 mM CTAC (hexadecyltrimethylammoniumchloride), pH 7.0
Capillary:	id=75 µm and BF 3 (225 µm pathlength); l=72 cm; L=80.5 cm
Injection:	200 mbar x s
E:	311 V/cm (negative polarity)
Temperature:	25 °C

Detection wavelength/bandwidth: Signal=300/16 nm, Reference=210/20 nm

in this case 75 µm BF 3 which has a 225-µm pathlength, improves detection but again has no significant effect on resolution. The bubble cell is also useful for detection of neutral solutes separated by micellar electrokinetic chromatography (MEKC). A representative example is shown in figure 7. Here a pH 8.9 borate phosphate buffer containing 100 mM SDS was used to

separate the components of Robitussin-CF cough syrup. Using the diode-array capabilities, the main peak was spectrally identified as guaifenesin. The increase in sensitivity with the bubble cell is especially useful since spectral identification and peak purity analysis are improved with increased signal-to-noise ratio.

25-µm id capillaries

The next series of experiments involved 25-µm id capillaries. As mentioned, these narrow capillaries are especially useful for the application of high electric fields and for use with highly conductive buffers without the detrimental effects of Joule heating. Detection difficulties with 25-µm capillaries arise not only from the short pathlength but also from the high ratio of outer-to-inner diameters (that is, thick walls). For these reasons the bubble cell inner diameter was increased to BF 5. The use of these capillaries for the MEKC analysis of six drug standards is shown in figure 8a and 8b. The advantage of the 5-fold increase in signal is evident. Importantly, the current generation dropped from 140, 60, to 14 µA when the internal diameter was reduced from 75 µm, to 50 µm, and 25 µm, respectively. Enlarging a section of the electropherograms enabled closer examination and comparison of the peak shapes from both the standard and bubble cell capillaries figure 8c. The first peak from each electropherogram, eluting at 4.6 minutes, was normalized to full scale and overlaid. It is evident that use of the bubble cell had no visible effect on the peak shape. Plate count analysis (using the width at half height method) showed that efficiencies calculated for both capillaries were around 200,000 plates/meter.

Detection limits

The final part of this work examines the detection limits of the diode-array using both standard and bubble cell capillaries. It is important to note that the diodearray detector does not require use of the bubble cell capillaries.

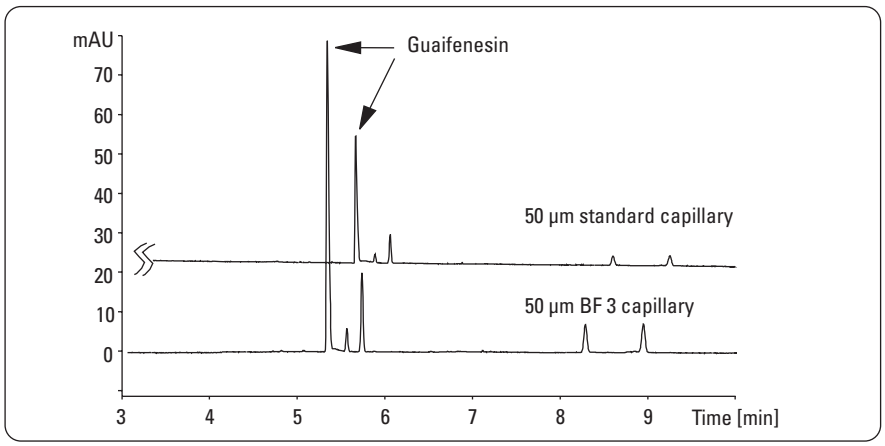

Figure 7
Standard and bubble cell capillaries for cold medication analysis by MEKC.

Chromatographic conditions

Sample:	1:20 dilution of Robitussin CF syrup (diluted in buffer)
Buffer:	11.7 mM borate, 8.3 mM phosphate, 100 mM SDS, pH 8.9
Capillary:	id=50 µm and BF 3 (150 µm pathlength); l=56 cm; L=64.5 cm
Injection:	200 mbar x s
E:	465 V/cm
Temperature:	37 °C

Detection wavelength/bandwidth = 214/16 nm

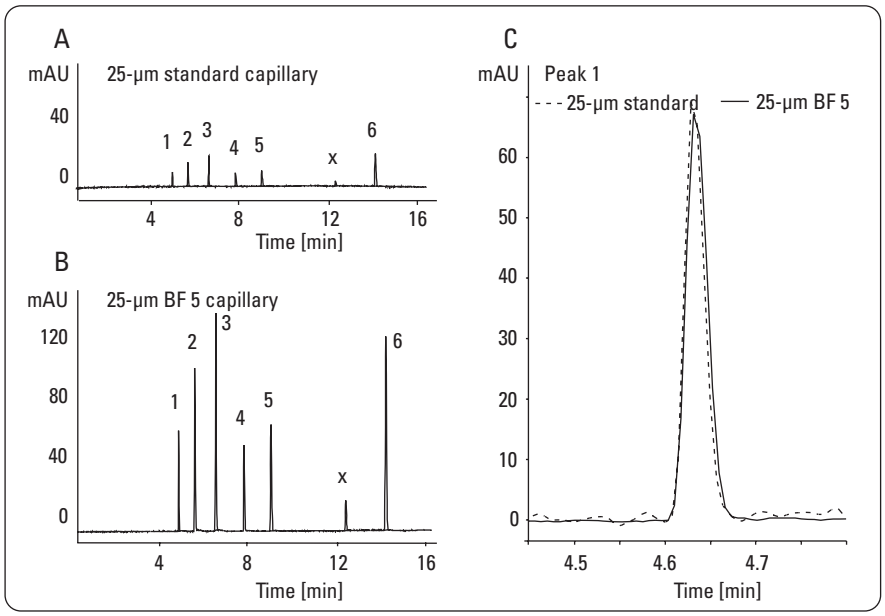

Figure 8
Comparison of 25-µm and 25-µm BF 5 capillaries in MEKC.

Chromatographic conditions

Sample:	1 = acetaminophen, 2 = caffeine, 3 = naproxen, 4 = guaifenesin, 5 = phenacetin, x = noscapine-related impurity, 6 = noscapine
Buffer:	11.7 mM borate, 8.3 mM phosphate, 100 mM SDS, pH 8.9
Capillary:	id=25 µm and BF 5 (125 µm pathlength) l=56 cm; L=64.5 cm
Injection:	200 mbar x s
E:	370 V/cm
Temperature:	37 °C

Detection wavelength/bandwidth = 200/16 nm

Detection limits with or without the bubble cell are simply proportional to the detection pathlength. For the purpose of measurement of detection limits, three representative solutes were chosen. The first was a dipeptide of composition Ala-Gly. This solute presented a significant challenge since the only chromophore is a single peptide bond. The results of injections of peptide concentrations at 5 µg/mL and 10 µg/mL using a 50 µm inner diameter capillary are shown in figure 9a. The signalto- noise ratios for the peptide peaks were 25 and 48, respectively. Extrapolating to a signal-to-noise ratio of 4 yielded a detection limit of 0.8 µg/mL.

In this work, standard CZE conditions were used and there was no attempt to increase sample concentration through isotachophoretic methods or overloading. The second experiment employed benzoic acid as a representative aromatic solute to measure detection limits. Figure 9b shows electropherograms of benzoic acid dissolved in water injected at concentrations down to 8 x10^{-8} M or 9.8 ppb. Here, a 75-µm BF 3 capillary with a detection pathlength of 225 µm was employed. The signal-to-noise ratio at this concentration was approximately 10 and is sufficient for accurate quantitative analysis and full use of the spectral capabilities of the DAD and ChemStation software.The third analysis employed indirect detection for inorganic anions. The separation of ppb levels of chloride, sulfate, and nitrate are shown in figure 9c. The buffer system consisted of a pyromellitic acid (1,2,4,5-benzenetetracarboxylic acid) as the UV-absorbing background electrolyte and hexamethonium hydroxide to reverse the EOF. With EOF reversal, solute migration and EOF were in the same direction, ensuring elution of all anionic solutes and shorter analysis time.

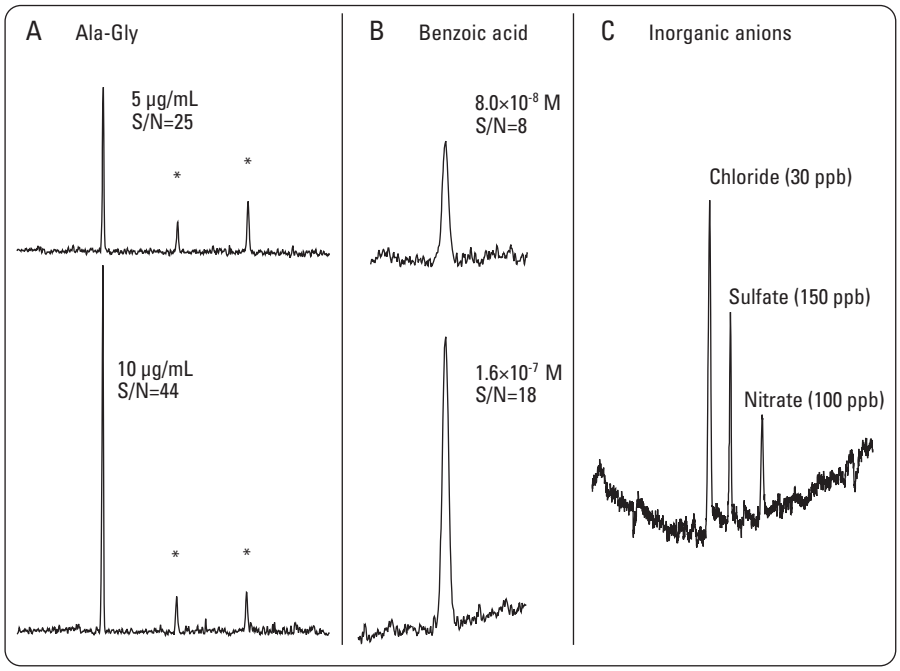

Figure 9
Representative diode-array detection limits.

Chromatographic conditions

Sample **A**:	dipeptide Ala-Gly in water
Buffer:	20 mM phosphate, pH 7.0
Capillary:	id=50 µm, l=40 cm, L=48.5 cm
Injection:	200 mbar x s
E:	619 V/cm
Temperature:	25 °C
Detection wavelength/bandwidth =200/16 nm	
(The peaks indicated by an asteris are impurities present in the diluent.)	
Sample **B**:	benzoic acid in water
Buffer:	20 mM borate, pH 9.0
Capillary:	id=75 µm and BF 3 (225 µm pathlength), l=56 cm, L=64.5 cm
Injection:	200 mbar x s
E:	465 V/cm
Temperature:	25 °C
Detection wavelength/bandwidth =200/16 nm	
Sample **C**:	chloride, sulfate, nitrate
Buffer:	2.25 mM pyromellitic acid, 6.6 mM NaOH, 0.75 mM hexamethonium hydroxide, 1.6 mM triethanolamine, pH 7.7
Capillary:	id=50 µm, l=56 cm, L=64.5 cm
Injection:	200 mbar x s
E:	465 V/cm (negative polarity)
Temperature:	25 °C
Detection wavelength/bandwidth: Signal=350/60 nm, Reference =245/10 nm	

Linear dynamic range

Accurate quantitative analysis over a wide range of solute concentrations requires a large linear detector range. This is important, for example, for the quantitative analysis of low level impurities in the presence of the main compound in a single run. Because the thickness of the capillary wall relative to the inner diameter is much smaller for the bubble cell than for a straight capillary, the potential for stray light is greatly reduced. As a consequence, the bubble cell offers an extended linear dynamic range. The linearity of the calibration curve for benzoic acid is shown in figure 10a. The system shows excellent linearity within the tested concentration range of 10 ppb to 100 ppm, with a correlation coefficient of 0.9991. Although the absorbance of the highest concentration of benzoic acid

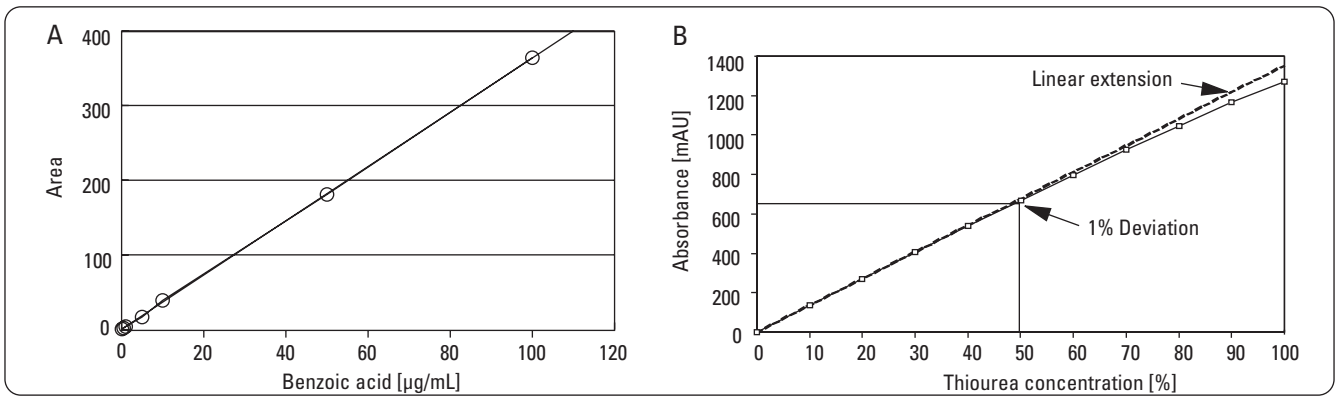

Figure 10
Calibration curves and determination of linearity.
The benzoic acid calibration curve was constructed using six benzoic acid concentrations ranging from 0.01 to 100 µg/mL. Each data point is the average of two replicate analyses. The linear dynamic range was determined from frontal analysis. The analyte is thiourea; dashed line corresponds to a linear extension of standard curve; solid line connects actual data points.

was 370 mAU, the linearity of the detector is shown in figure 10b to be beyond 600 mAU, as shown in the next example. Perhaps a more accurate method for determining detector linearity is based on decoupling all the other factors that introduce variability from the detector response by performing frontal analysis. In this procedure, step functions of increasing analyte concentration are flushed past the detector until the absorption of each reaches a steady-state. This provides an accurate measure of absorption as a function of concentration. Results from frontal analysis using various concentrations of thiourea in a 50-µm BF 3 capillary are shown in figure 10b. The linearity, as defined by a 1 % deviation from the linear extension of the standard curve, was 650 mAU with this system.

Conditions
Capillary: id=50 µm and BF 3 (150 µm pathlength)
Detection wavelength/bandwidth = 235/5 nm

Conclusion

The design and operation of bubble cell capillaries is described. The capillaries yielded a 3-to 5-fold increase in sensitivity relative to standard capillaries. Used with 25-µm id capillaries, they offered a solution to the detection difficulties normally inherent with narrow internal diameter capillaries. Detection limits of below 10 ppb were demonstrated for aromatic compounds, below 1 ppm for simple dipeptides, and in the lowto- mid ppb range for inorganic anions by indirect UV detection. Additional advantages included improved detector linearity, which exceeded 600 mAU and over five orders of magnitude concentration.

Reference

1
D. N. Heiger, P. Kaltenbach, H.-J. P. Sievert, “Diode array detection in capillary electrophoresis,” *Electrophoresis, , 15 (1), 1234-1247* **1994.**

www.agilent.com/chem/ce

Published March 1, 2009
Publication Number 5990-3410EN

Agilent Technologies